Fibroin Silk Synthesis and Fabrication of Silk Fibroin/Graphene Oxide Nano-Sheet Film for Humidity Sensing

Shima Haghgooyan, Fatemeh Ostovari*, Hakimeh Zare, and Zahra Shahedi

Department of Physics, Yazd University, Yazd, Iran

***Corresponding author email**: ostovari@yazd.ac.ir

Regular paper: Received: Mar. 24 2022, Revised: Jul. 15, 2022, Accepted: Jul. 22, 2022,
Available Online: Jul. 24, 2022, DOI: 10.52547/ijop.16.1.19

ABSTRACT— Silk fibroin (SF) is a natural material that has received special attention due to its excellent mechanical and electrical properties. Nowadays, it is tried to improve the properties of SF by adding other nanomaterials such as graphene oxide (GO). Here, we extracted SF from silk cocoon and studied its properties in pure state and in the combination with graphene oxide (SF/GO). The results have shown that the presence of graphene oxide in the structure of fibroin increases the random winding formation of SF. The measurements show that the water content has a great effect on the properties of SF and SF/GO films. The contact angle (less than 70) indicates the hydrophilic property of these films. In addition, in times greater than 50 seconds, the contact angles drop to 27° and 5° for SF and SF/GO respectively. Also, the surface resistance of the completely dried SF/GO film increases from 50 kW/sq to 220 kW/sq for 42% wt water content.

KEYWORDS: Silk fibroin, Graphene Oxide Nano-sheet, surface resistance, water content, Humidity sensitive.

I. INTRODUCTION

In recent decades, we have witnessed the rapid development of flexible electronics through leaps in the marketplace and the publication of a variety of devices, containing flexible actuators, flexible cells, flexible displays, flexible integrated electronics microsystems, as well as coverage. We see comprehensive applications in the fields, including technology, energy, and health care [1-6]. Among the most widely used flexible materials: polytetrafluoroethylene, polydimethylsiloxane (PDMS), polyamide, fluorinated ethylene-propylene, and silicone rubber, due to their reproducible mechanical properties, in the long run, the action of the main role in achieving the flexibility and/or elasticity of electronic devices [2, 7]. One of the most promising materials for flexible electronic devices for future generations is biological materials [8, 9]. In this regard, also, SF due to its various functional features, has the unique advantage of solving the problem of stable power supply and flexible electronic multifunction integration. These advantages, combined with lightweight and transparency, as well as ease of processing, make SF open a new path in the realm of flexible electronics [7-13].

In this study, a moisture sensor was fabricated using SF as a substrate and GO as a functional sensor material interestingly, GO /SF acts as an essential component of wearable devices.

II. EXPERIMENTS

A. *Materials and Methods*

In this study, silkworm cocoons, sodium bicarbonate, calcium chloride, ethanol, deionized water, potassium permanganate, graphite powder, sulfuric acid, sodium nitrate, hydrochloric acid, Hydrogen peroxide (H_2O_2), and formic acid without additional purification were used.

To evaluate the results, the FTIR Vertex 70 infrared spectrometer was used to record the

[Downloaded from ijop.ir on 2026-11-23]

FTIR spectrum, and the visible ultraviolet electron spectroscopy was used to record the UV-Vis spectra. Also, to study the morphology of the samples, the SEM scanning electron microscope of Yazd University and the TEM electron image were used. To record the structure of the samples, x-ray diffraction (XRD) was used to study the structure and to form crystals. Raman spectroscopy was used to determine the chemical structure and material detection.

B. *Preparation of SF Solution*

The process of preparing an SF solution in four main steps can be summarized. As shown in Fig .1 (a), first, the silkworm is extracted from cocoons. To remove sericin, (1) an amount of Bombyx cocoon is cut into small pieces for better dispersion. (2) Prepare a solution of 0.02 M sodium carbonate (Na_2CO_3) add the cocoon pieces to the boiling Na_2CO_3 solution and boil for 30-45 minutes to remove sericin. Finally, to remove the remaining sericin (3) the extracted silk fibers are washed more than four times in deionized water (DI). (4) Dried SFs are obtained by pressing excess water and drying them naturally or in an oven. In the second step, a 9 M solution of calcium chloride ($CaCl_2$) is prepared in advance and added to the SFs in a glass and then placed in a hot plate at 50 ° C for 4 hours until the SFs are completely dissolved. In the third step, the silk/calcium chloride mixture solution is injected through a syringe into one of the dialysis films and dialyzed against DI water for 72 hours to remove CaCl2 ions to obtain the SF solution. It should be noted that DI water should be replaced several times during the dialysis process. Finally, the SF solution is centrifuged twice at 9000 rpm for 20 minutes to eliminate impurities. It is then stored in an environment below 4 °C to perform analysis and fabrication to reduce the gelling effect of the solution [14, 15].

C. *Preparation of GO*

To fabrication, GO from the Hummers method was used to oxidize graphite powder (Fig. 1 (b)). For this aim, 2 g of $NaNO_3$ and 3 g of graphite were blended with 74 ml of H_2SO_4 in a 250 ml flask. Then, the flask was placed in an ice bath for 20 min to cool to 7-11 °C. Next, 4.5 g of $KMnO_4$ was slowly added to the flask. The temperature at this stage was kept at 35 °C for 35 min. Then, 92 ml of DI was added to dilute the solution. After 20 min, 360 ml of H_2O_2 solution was added to the flask. The product was obtained by filtration, washed with DI and HCl, and dried at 70 °C for 24 h to obtain graphite oxide powder. To obtain graphene oxide, the product is ultrasonic for 4 hours [16-18].

D. *Production of SF/GO Films*

In recent years, flexible electronic devices have become very popular due to their excellent flexibility, lightweight, and controllable transmission. In this regard, flexible films such as SF are used more because of advantages such as ease of preparation and low cost.

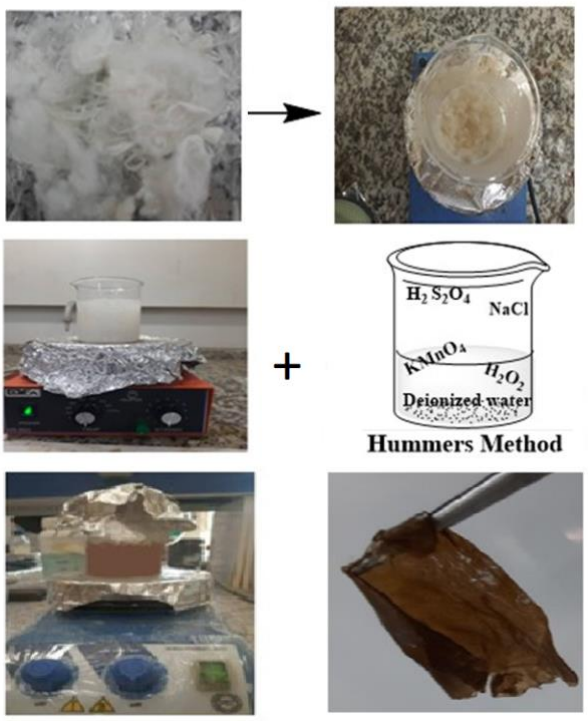

Fig. 1. Schematic of synthesis steps fibroin, graphene oxide and fibroin / graphene oxide.

First, an SF/ GO solution is prepared and dispensed directly on the surface of a smooth substrate, such as a plastic petri dish coating. To prevent denaturation, SF/GO films are usually dried at room temperature. Finally, the dried SF films are immersed in an alcoholic

[Downloaded from ijop.ir on 2026-11-23]

solution or a water vapor medium to crystallize and achieve better mechanical properties as well as optimum degradation rates (Fig. 1 (c)).

III. Results and Discussion

Figure 2(a) shows a microscope image passing through graphene oxide nano-sheets. As can be seen, graphene oxide is quite clear and has a low level. The low level of graphene oxide is due to the accumulation of graphene oxide sheets during the drying operation because the Van der Waals force between each sheet is unavoidable. The graphene oxide phases using X-ray diffraction are shown in Fig. 2(b). According to the figure, the XRD spectrum of graphene oxide has a tall peak at an angle of 10.21° with the plane (001), which is a specific peak available for graphene oxide. Also, a weak peak is observed at an angle of 22° with the plane (002), which is due to the presence of low impurities in graphene oxide powder and is due to graphite remaining in the sample, which is very small in size and amorphous or concentrated and or in the effect of the very high concentration of graphite does not appear to be characteristic and can only be caused by turbulence. According to Fig. 2 (c), the identification of functional groups in pure graphene oxide has been done by FTIR spectrum in the range of 400-4000cm^{-1}. The FTIR spectrum of graphene oxide shows the presence of C=O bond in the range of 1730 cm^{-1}, C-OH at 1420 cm^{-1}, C-O in the range of 1050 cm^{-1}, and C-O-C cm^{-1} in the range of 1250 cm^{-1} and C-C in the range of 1600 cm^{-1}. Fig 2(d) shows the Raman spectrum of graphene oxide nano-sheets. Raman spectroscopy is the most important method for structural and electronic characterization of graphene oxide nano-sheets. The G-band for graphene oxide in this range confirms the formation of new Sp^3 carbon atoms. Also, the increase or decrease of the D band in the range of 1300 cm^{-1} is due to the decrease or increase in the size of Sp^2 domains within graphite plates. All changes in graphene oxide Raman spectra compared to graphite are mainly due to the oxidation process and depend on the graphite crystal lattice [14, 19].

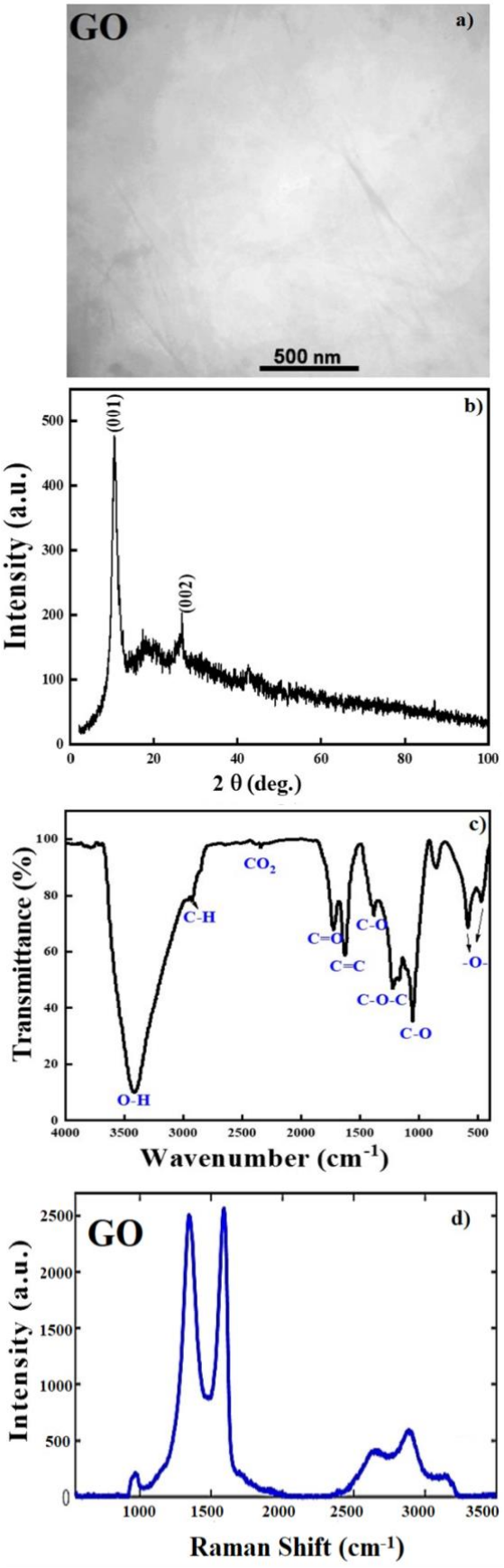

Fig. 2 a) TEM image b) X-ray diffraction c) FTIR spectroscopy and d) Raman spectroscopy of graphene oxide.

[Downloaded from ijop.ir on 2026-11-23]

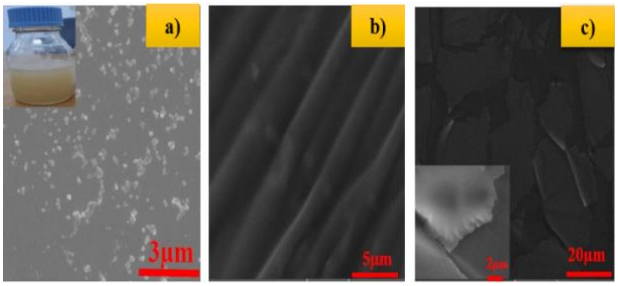

Fig. 3. SEM images of a) SFs, b, c) SF / GO films.

SEM images are mainly used to study the morphology and mess in the structure of nanoparticles with bulky samples on the surface. Figure 3 (a), (b), and (c) show the morphology of the solution in the form of fibroin films and fibroin/graphene oxide films prepared using SEM. The morphology of silk nanoparticles was investigated using SEM in Fig. 3 (a). All particles made of silk have a spherical shape. Time is effective in preparing the solution on the particles and in the maximum optimal time of 90 minutes, it leads to the most uniform particles (smaller than 100 nm) and is independent of the production method. As can be seen in Figs. 3 (b) and (c), the images show the thin, and flat, uniform shape SF/GO film.

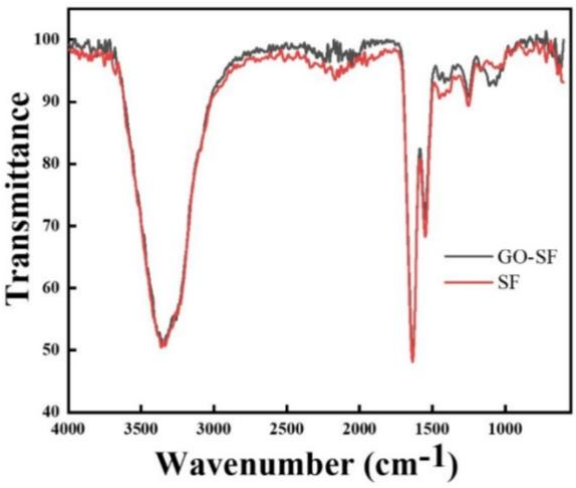

Fig. 4. The FTIR spectrum shows the region of amide I, II, and III in solutions pure of silk fibroin and SF / GO nanocomposites.

Figure 4 shows the FTIR spectrum of SF and graphene oxide/SF. In the FTIR spectrum of silk fibroin, the peak of 711 cm^{-1} is related to CH_2 bending, 1071 and 1454 cm^{-1} are related to C-N stretching bond, peak 1254 cm^{-1} is related to N-H bond, peak 1419 cm^{-1} is related to C-O-H, 1545 cm^{-1} is related to amide II and 1640 cm^{-1} is related to amide I, 2940 cm^{-1} are related to CH_3 and CH_2 stretching bond, 3079 cm^{-1} are related to CH stretching bond in CH-CH_2 and peak 3249 and 3340 cm^{-1} are related to NH and OH bonds, respectively [9,10]. If amide I is in the range of 1630-1610 cm^{-1} and amide II is in the range of 1510-1520 cm^{-1}, it shows the secondary structure of silk II, and if amide I is in the range of 165-1654 cm^{-1} and amide II is in the range of 164-1654 cm^{-1}, showing the secondary structure of silk I, so according to the peaks of amide I and II, it can be concluded that the secondary structure of fibrin used is the silk I. As can be seen in the SF/GO spectrum, amide I and amide II bands for slightly modified Schiff nanocomposite solutions, which indicate a deformation into a spiral or random winding. The integration of graphene oxide Nano-sheets in silk fibroin solution reduces β-sheets and increases the random winding composition [20-22]. Silk fibroin chains have intramolecular or intermolecular interactions due to the acidic conditions in which the molecules are entangled. The integration of graphene oxide nano-sheets disrupts the chain-to-chain interaction in solution, increasing the randomization of silk fibroin nanocomposite solutions.

The functional groups and bands of SF, GO and SF / GO were examined using a UV-vis spectrophotometer with their solutions (Figure 5). As can be seen from Fig. 5(a) the peaks of nitrotyrosine are observed at wavelengths of 234, 273, and 400 nm. Absorption peaks at about 220 and 295 nm for graphene oxide (Fig. 5(b)) indicate the GO nano-sheets. The absorption peak at 230 is related to the C-C bond, and the peak at 295 nm is related to the C=O bond. In the SF / GO solution (Fig. 5(c)) all peaks of graphene oxide and fibroin are observed.

To investigate the effect of water content, the dried film weight is measured, and its strength is checked qualitatively .To perform the effect of water content, the dry film weight and strength are measured and then the film is measured at different times of dry and sheet

[Downloaded from ijop.ir on 2026-11-23]

strength. When the quality of the film does not change, the film is put in the oven and dry at 90 °C for 2 hours and it is a film with zero humidity. The water content can be calculated at different times with the following formula.

$$\text{Water content (\%)} = (M_1\text{-}M_2)/M_1\times 100 \qquad (1)$$

where M_1 and M_2 are the weight of the SF/GO film and its completely dried weight at 90° for 2 hours, respectively.

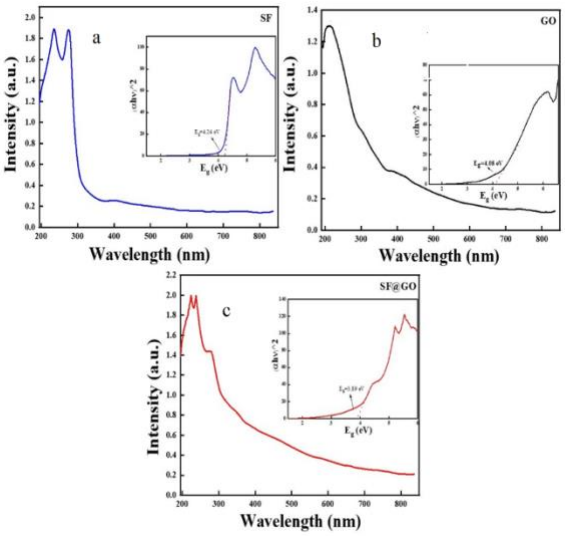

Fig. 5. UV-vis spectroscopy results of solutions a) SF, b) GO and c) SF / GO along with calculation of band gap of samples

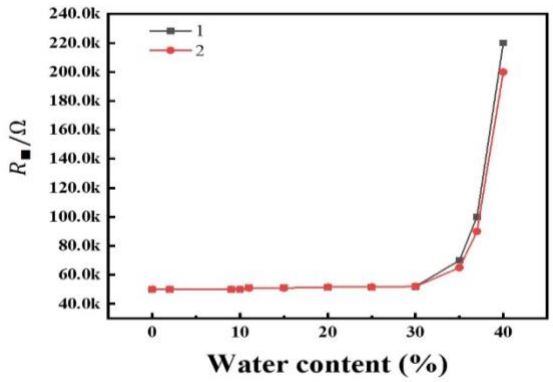

Fig .6. Graph of surface resistance vs water content percentage for SF/GO film.

Figure 6 shows a diagram of the film surface resistance curve in terms of water content for two consecutive times.

A four point-probe aperture, digital I-V meter and microvoltmeter was used for measurement of surface resistance. The I-V meter utilized to generate current and microvoltmeter was used to measure the voltage difference between two tips. They connect to related probes by alligator clips. Then the sheet resistivity of the sample is calculated using $\rho = 4.25\ V/I$ for different water content percentage.

The properties of polymeric materials strongly depend on the water content. As can be seen, the resistance of SF/GO films increases with increasing water content. When the water content is 0%, the surface resistance is 50 kW/sq and when the water content is close to 42%, the resistance reaches 220 kW/sq, which indicates an increase of several hundred times the resistance of the film. When the water content is reduced and fibroin is recovered, the distance between the graphene sheets is also restored and the electrical resistance is reduced by retesting. As a result, this material has great potential in the field of moisture-sensitive sensors [23] with suitable repeatability because of the water content control by heating.

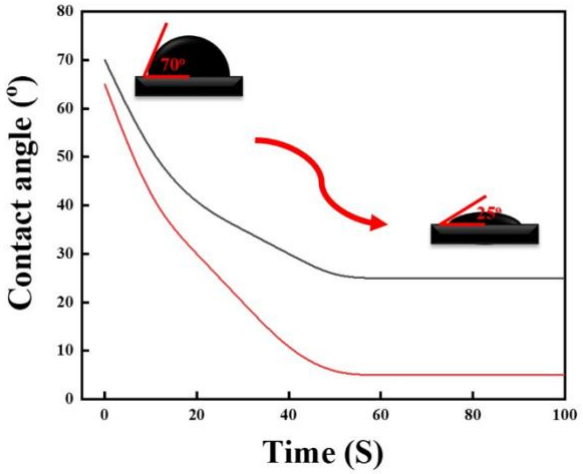

Fig. 7. Temporal evaluation of water contact angle in SF and SF / GO films

The hydrophilic properties of SF can affect the ability of layers to absorb water. As shown in Fig. 7, the contact angle of a drop of water on the dried SF film is only 70° and quickly dropped to 27° in 50 to 100 seconds, which is due to good hydrophilicity and high-water absorption. This indicates that SF films react rapidly to changes in humidity. In addition, SF films have a very smooth surface and therefore a uniform film thickness, which is desirable for displaying bright colors. The contact angle of

[Downloaded from ijop.ir on 2026-11-23]

a drop of water on the SF/GO film is only 65° and quickly dropped to 5° in 50 to 100 seconds, which is due to good hydrophilicity, porosity created by graphene sheets within the SF, and high-water absorption.

IV. CONCLUSION

SF Fibroin Silk has many superior properties, including remarkable biocompatibility, adjustable biodegradability, and water solubility, excellent optical transmission, good mechanical strength, lightweight, and ease of processing which makes it suitable for the next generation of biocompatible flexible makes it very convenient. Due to their desirable biological properties, SF is widely used as an essential component, e.g., substrates and enclosures, as well as scaffolding, flexible wearable, and implantable electronic devices, such as electronic skins, bio-absorbable electronics, and electronics therapy, can be used. In this study, first, fibroin from silkworm cocoons and graphene oxide nano-sheets by the Hammers method were prepared. Then, fibroin/graphene oxide composite film was prepared by simple combination and casting method. The structure of the film was characterized by FTIR, and SEM and its electrical and optical properties were investigated. The properties of fabricated graphene oxide nano-sheets were also discussed. The results showed that the resistance of the film is related to the water content, which can be used as a humidity sensor. Due to the SF sensitivity characteristics to environmental variables, many flexible sensors with functional SF such as humidity, temperature, pressure, airflow, and electrochemical sensors are recommended.

REFERENCES

[1] C. Wang, K. Xia, H. Wang, X. Liang, Z. Yin, and Y. Zhang, "Advanced carbon for flexible and wearable electronics," Adv. Mater. Vol. 31, pp. 1801072 (1-37), 2019.

[2] M.K. Filippidou, E. Tegou, V. Tsouti, and S. Chatzandroulis, "A flexible strain sensor made of graphene nanoplatelets/ polydimethylsiloxane nanocomposite," Microelectron. Eng. Vol. 142, pp. 7–11, 2015.

[3] H. Lee, T.K. Choi, Y.B. Lee, H.R. Cho, R. Ghaffari, L. Wang, H.J. Choi, T.D. Chung, N. Lu, and T. Hyeon, "A graphene-based electrochemical device with thermoresponsive microneedles for diabetes monitoring and therapy," Nat. Nanotechnol. Vol. 11 pp. 566-572, 2016.

[4] K. Xia, C. Wang, M. Jian, Q. Wang, and Y. Zhang, "CVD growth of fingerprint-like patterned 3D graphene film for an ultrasensitive pressure sensor," Nano Res. Vol. 11, pp. 1124–1134, 2018.

[5] D.H. Ho, Q. Sun, S.Y. Kim, J.T. Han, D. H. Kim, J. H. Cho, "Stretchable and multimodal all graphene electronic skin," Adv. Mater., Vol. 28, pp. 2601–2608, 2016.

[6] S. Wang, Z. Chen, A. Umar, Y. Wang, T. Tian, Y. Shang, Y. Fan, Q. Qi, D. Xu, "Supra molecularly modified graphene for ultrafast responsive and highly stable humidity sensor," J. Phys. Chem., Vol. 119, pp. 28640–28647, 2015.

[7] D. T. Pham, & W. Tiyaboonchai, "Fibroin nanoparticles: A promising drug delivery system," Drug delivery, Vol. 27(1), pp. 431-448, 2020.

[8] H. Huang, H. Guiying, X. Ke, W. Qin, W. Di, Y. S. Matthew, and X. Jianlong, "Achieving long-lived triplet states in intramolecular SF films through molecular engineering," Chem. Vol. 5, pp. 2405-2417, 2019.

[9] S. Li, L. Li, G. Chengrui, Q. Huanhuan, and Y. Xixun, "A promising wound dressing material with excellent cytocompatibility and proangiogenesis action for wound healing: Strontium loaded Silk fibroin/Sodium alginate (SF/SA) blend films," International journal of biological macromolecules, Vol. 104, pp. 969-978, 2017.

[10] G. Freddi, T. Masuhiro, and B. Silvia, "Structure and physical properties of silk fibroin/polyacrylamide blend films," J. Appl. Polymer Science, Vol. 7, pp. 1563-1571, 1999.

[11] C.S. Shivananda, R. Madhu Kumar, B. Narayana, K. Byrappa, P. Renu, Youjiang Wang, and Y. Sangappa, "Preparation and characterisation of silk fibroin–silver nanoparticles (SF–AgNPs) composite films," Mater. Research Innov. Vol. 21, pp. 210-214, 2017.

[Downloaded from ijop.ir on 2026-11-23]

[12] G.R. Shetty and B.L. Rao, "Preparation, characterization of SF-HPMC blend films and SF microparticles," Mater. Today: Proc. Vol. 49, pp.1822-1826, 2015.

[13] G. Perotto, Y. Zhang, D. Naskar, N. Patel, D. L. Kaplan, S.C. Kundu, and F.G. Omenetto, "The optical properties of regenerated silk fibroin films obtained from different sources," Appl. Phys. Lett. Vol. 111, pp.103702 (1-4), 2017.

[14] R. Yadav, B. Radhika, B. Priya, and P. Roli, "N-type silk fibroin/TiO_2 nanocomposite transparent films: electrical and optical properties," Polymer International, Vol. 71, pp. 74-85, 2022.

[15] Y. Zheng, W. Lili, Z. Lianjia, W. Dongyi, X. Hao, W. Kang, and H. Wei, "A Flexible Humidity Sensor Based on Natural Biocompatible Silk Fibroin Films," Adv. Mater. Technol. Vol. 6, pp. 2001053 (1-8), 2021.

[16] M. Rasheed, S. Shihab, and O.W. Sabah, "An investigation of the Structural, Electrical and Optical Properties of Graphene-Oxide Thin Films Using Different Solvents," J. Phys.: Conference Series, Vol. 1795, pp. 012052 (1-12), 2021.

[17] F. Ostovari, Y. Abdi, and F. Ghasemi, "Controllable formation of graphene and graphene oxide sheets using photo-catalytic reduction and oxygen plasma treatment," The Europ. Phys. J.-Appl. Phys. Vol. 60, pp. 30401 (1-6), 2012.

[18] M. Joghataei, F. Ostovari, S. Atabakhsh, and N. Tobeiha. "Heterogeneous ice nucleation by Graphene nanoparticles," Scientific Reports, Vol. 10, pp. 1-9, 2020.

[19] M.T.U. Malik, A. Sarker, S.S.M. Rahat, and S.B. Shuchi, "Performance enhancement of graphene/GO/rGO based supercapacitors: A comparative review," Mater. Today Commun. No. 102685, pp. 102685 (1-7), 2021.

[20] A. Reizabal, C.M. Costa, P.G. Saiz, B. Gonzalez, L. Pérez-Álvarez, R.F. de Luis, and S. Lanceros-Méndez, "Processing Strategies to Obtain Highly Porous Silk Fibroin Structures with Tailored Microstructure and Molecular Characteristics and Their Applicability in Water Remediation," J. Hazardous Mater. Vol. 403, pp. 123675 (1-30), 2021.

[21] Z. Chen, Q. Zhang, H. Li, Q. Wei, X. Zhao, and F. Chen, "Elastin-like polypeptide modified silk fibroin porous scaffold promotes osteochondral repair," Bioactive Mater. Vol. 6, pp. 589-601, 2021.

[22] Y. Liang, A. Mitriashkin, T.T. Lim, and J.C.H. Goh, "Conductive polypyrrole-encapsulated silk fibroin fibers for cardiac tissue engineering," Biomater. Vol. 276, pp. 121008 (1-14), 2021.

[23] H. Zhang, J. Zhao, T. Xing, S. Lu, and G. Chen, "Fabrication of silk fibroin/graphene film with high electrical conductivity and humidity sensitivity," Polymers, Vol. 11, pp. 1774 (1-12), 2019.



Shima Haghgooyan is student of M.Sc. in solid State Physics, from Yazd University, Yazd, Iran. Her main interests include nano-physics, and nano-biophysics.



Fatemeh Ostovari received her Ph.D. in Physics from the Tarbiat Modares University, Tehran, Iran., in 2014. Dr. Ostovari has been a tenured member of Physics Department, Yazd University, Yazd, Iran, ever since. Her main interests include nano-optoelectronic, nanophysics, and nano-biophysics.

[Downloaded from ijop.ir on 2026-11-23]



Hakimeh Zare received her Ph.D. in Nanotechnology from the Sharif University of Technology, Tehran, Iran., in 2015. Dr. Zare has been a tenured member of Physics Department, Yazd University, Yazd, Iran, ever since. Her main interests include nano-optoelectronic, nano-physics, and nano-biophysics.



Zahra Shahedi received her Ph.D. in Physics from the Arak University, Arak, Iran. In 2017. Her main interests include nano-optoelectronic, nano-physics, and nano-biophysics.

[Downloaded from ijop.ir on 2026-11-23]